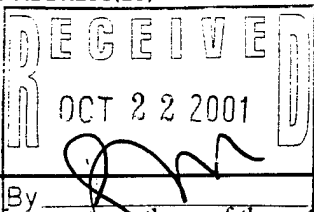


REPORT DOCUMENTATION PAGE			Form Approved OMB No. 0704-0188	
Public reporting burden for this collection of information is estimated to average 1 hour per response, including the time for reviewing instructions, searching existing data sources, gathering and maintaining the data needed, and completing and reviewing the collection of information. Send comments regarding this burden estimate or any other aspect of this collection of information, including suggestions for reducing this burden, to Washington Headquarters Services, Directorate for Information Operations and Reports, 1215 Jefferson Davis Highway, Suite 1204, Arlington, VA 22202-4302, and to the Office of Management and Budget, Paperwork Reduction Project (0704-0188), Washington, DC 20503.				
1. AGENCY USE ONLY (Leave blank)	2. REPORT DATE 15 January 1998	3. REPORT TYPE AND DATES COVERED Final 10 Jul 95-09 Aug 97		
4. TITLE AND SUBTITLE Materials Research Center of Excellence		5. FUNDING NUMBERS DAAH04-95-2-0006 Formerly DAAH04-94-G-0316		
6. AUTHOR(S) Dr. James Wagner				
7. PERFORMING ORGANIZATION NAME(S) AND ADDRESS(ES) Johns Hopkins University Department of Materials Science & Engineering 3400 North Charles Street Baltimore, MD 21218		8. PERFORMING ORGANIZATION REPORT NUMBER		
9. SPONSORING/MONITORING AGENCY NAME(S) AND ADDRESS(ES) U.S. Army Research Office PO Box 12211 Research Triangle Park, NC 27709-2211		10. SPONSORING/MONITORING AGENCY REPORT NUMBER 34817-MS V •1		
11. SUPPLEMENTARY NOTES The views, opinions and/or findings contained in this report are those of the author(s) and should not be construed as an Official Department of the Army position, policy or decision, unless so designated by other documentation.				
12a. DISTRIBUTION AVAILABILITY STATEMENT Approved for public release: distribution unlimited.				
20011101 025				
13. ABSTRACT (Maximum 200 words) This report details results from a program supported through the ARO to establish technical collaborative links between investigators at the Johns Hopkins University and their technical counterparts at the Army Research Laboratories/Materials Directorate. With technical program guidance primarily from Dr. James McCauley, eight research tasks were pursued. For each task an investigator at the ARL Materials Directorate provided guidance and, in many cases, close collaboration toward achieving the research task goals. Each of these programs has built collaborative interaction between JHU and ARL and, we hope, has formed the basis for a long term collaborative interaction. In addition to the eight research tasks supported, the program has made accommodation for seven ARL researchers to be housed at the Johns Hopkins Homewood campus. Both office space and designated laboratory space are occupied and used by these researchers. Among these visiting scientists are principal collaborators for three of the research tasks. Three ARL/MD scientists also have matriculated as PhD candidates in the Johns Hopkins Department of Materials Science and Engineering. Thus, a total of ten ARL scientists have been housed on-site at Johns Hopkins.				
14. SUBJECT TERMS Corrosion Protection, Compliant Smart Materials, Metal Matrix Composites, Tungsten Penetrators, Nondestructive Evaluation, Chemical Barrier Elastomers, Silicon Surface Modification, Processing of Ductile Iron.			15. NUMBER OF PAGES 37	
			16. PRICE CODE	
17. SECURITY CLASSIFICATION OF REPORT UNCLASSIFIED	18. SECURITY CLASSIFICATION OF THIS PAGE UNCLASSIFIED	19. SECURITY CLASSIFICATION OF ABSTRACT UNCLASSIFIED	20. LIMITATION OF ABSTRACT UL	

Materials Research Center of Excellence

**Contract No. DAAH04-95-2-0006
(Formerly Contract No. DAAH04-94-G-0316)**

Final Technical Report

15 January 1998

Submitted to:

**U. S. Army Research Office
AMXRO-MS
Research Triangle Park, NC 27709-2211**

**James W. Wagner
Department of Materials Science and Engineering
Johns Hopkins University
Baltimore, MD 21218**

Table of Contents

	Page No.
Introduction	1
Tasks	2
Corrosion Effects and Protection of Alloys	3
PI's: J. W. Wagner and P. C. Searson	
Compliant Smart Materials	13
PI's: A. S. Douglas and K. T. Ramesh	
Interface and High Temperature Property Measurements for Metal Matrix Composites	15
PI's: M. Rosen and J. B. Spicer	
Adiabatic Shear Localization in Body-Centered Cubic Metals	24
PI's: K. T. Ramesh and K. J. Hemker	
Nondestructive Characterization of Polymer Matrix Composite Materials	26
PI's: R. E. Green, Jr., J. W. Wagner, J. B. Spicer, and J. M. Winter	
Diffusion of Vapor Mixtures through Elastomers	29
PI: T. Barbari	
Characterization and Modification of Silicon Surfaces at Liquid Interfaces	30
PI: P. C. Searson	
Process Monitoring and Control in the Production of Austempered Ductile Iron	36
PI: J. B. Spicer	

Materials Research Center of Excellence
Contract No. DAAH04-95-2-0006
(Formerly Contract No. DAAH04-94-G-0316)

Final Technical Report

Introduction

This report details research activities undertaken through the second year of a program supported through the ARO to establish technical collaborative links between investigators at the Johns Hopkins University and their technical counterparts at the Army Research Laboratories/Materials Directorate. With technical program guidance primarily from Dr. James McCauley, eight research tasks were pursued. For each task an investigator at the ARL Materials Directorate provided guidance and, in many cases, close collaboration toward achieving the research task goals. Each of these programs has built collaborative interaction between JHU and ARL and, we hope, has formed the basis for a long term collaborative interaction.

In addition to the eight research tasks supported, the program has made accommodation for seven ARL researchers to be housed at the Johns Hopkins Homewood campus. Both office space and designated laboratory space are occupied and used by these researchers. Among these visiting scientists are principal collaborators for three of the research tasks. Three ARL/MD scientists also have matriculated as PhD candidates in the Johns Hopkins Department of Materials Science and Engineering. Thus, a total of ten ARL scientists have been housed on-site at Johns Hopkins.

Technical Progress

The pages which follow provide brief descriptions of research progress made in each of the technical research task areas. Also identified for each task are the names of the principal investigators at Johns Hopkins and the technical points of contact at the ARL/Materials Directorate. In most cases, technical interchange beyond what is contained in this report has taken place between ARL and JHU personnel.

TASKS

Corrosion Effects and Protection of Alloys

Principal Investigators: J. W. Wagner and P. C. Searson
Technical Point of Contact: J. Beatty

Objectives

The objectives of this task were two-fold. However, both aspects were intended to help study and explain corrosion behavior. The first objective was to employ advanced acoustic emission techniques to attempt to differentiate between types of environmentally dependent fracture mechanisms in aluminum alloys. The second objective was to characterize the effectiveness and breakdown of conversion coatings for the protection of aluminum alloys.

Research Accomplishments

Acoustic Emission Evaluation of Environmentally Assisted Cracking

Background

Environmentally assisted cracking (EAC) is a significant problem in modern structures. The combination of a susceptible material, an adverse environment, and mechanical stress can lead to unexpected failure of a structure by catastrophic crack growth. Additionally, the operating environment of the U.S. Army contributes to premature failure of structures such as aluminum alloy armor, high strength steel armor, and high strength steel control components on Army helicopters. These failures not only endanger life, but they also seriously hamper the fighting readiness of U.S. forces due to equipment down time for inspection and repair of faulty components. Work has been performed to better characterize EAC resistance in high strength aluminum armor alloys. These high strength alloys are particularly prone to failure in a chloride environment - an environment encountered in most of the world. To avoid such failures, we must better understand the EAC phenomena and more diligently detect growing cracks before they become critical in length. One characterization technique that promises to serve well both as a laboratory tool for understanding EAC and as a field device for detecting EAC is acoustic emission evaluation. This promise is borne of the inherent nature of cracking phenomena. When a material cracks, even on a microscopic level, it releases energy in the form of mechanical waves. These waves travel throughout the structure. Acoustic emission (AE) is the science of monitoring these waves and determining the nature and significance of the event that caused them. Usefulness of AE depends on three general abilities. First, can surface disturbance be measured accurately? Second, can we understand how the mechanical wave is transformed on its journey from source to receiver? Third, can we accurately describe the source of the mechanical wave given the previous abilities coupled with our theoretical know-how? In answering these questions sufficiently, we will find that AE can be useful in characterizing and preventing EAC in engineering structures. The limits within which AE can be useful has been the goal of this research endeavor.

Theoretical Considerations

A full discussion of the theoretical issues associated both with the nature of the environmentally assisted cracking phenomenon and the ability to detect distinguishing features of the acoustic emissions resulting from crack propagation by various cracking phenomena is contained in a masters thesis produced by Paul Buckley as a result of this study. That manuscript has been provided to the ARO as part of this reporting process and is available for more detailed review. In summary, however, the theoretical issues to be understood include the nature of environmentally assisted cracking, mechanisms by which acoustic emission is generated and propagated, and the means for accurate sensing of the acoustic emission wave and determination of its source location.

With regard to the issues of the nature of environmentally assisted cracks and the mechanisms by which they may produce emissions, there were three models considered. The first was a hydrogen embrittlement phenomenon in which hydrogen is assumed to diffuse to the crack tip area, thus embrittling the material and leading to rapid and localized crack growth. The second phenomenon considered was that involving brittle rupture of a passive film formed near the crack tip. A third model assumes a more continuous synergy between corrosion and tensile stress at a crack tip allowing for crack advance. Elastic waves released from any of these phenomena occur when there is a sudden localized change in the stress state. The more dramatic the change, the greater likelihood that the wave thus generated can be easily detected. It is reasonable to model the source of these waves as a point given the relatively long distance of the wave propagation path compared with the size of the source itself. This source will produce a wave that will travel throughout the material until detected at some receiving point. The displacement at the detection point can be predicted theoretically by convolution of the source function with the transfer function affecting the elastic waves in the given material.

The morphology or amplitude pattern of the acoustic emission will vary depending upon the source type. Consider, for example, a growing crack still joined by a ligament. Upon fracture of the ligament, two fracture surfaces will separate and act as two half spaces with their representative equal and opposite point forces creating elastic waves. The compressional wave amplitude thus generated will have an angular dependence which can be predicted by a double monopole consisting of two equal and opposite forces. Still other crack mechanisms may give rise to a dilatational source radiating uniformly in all directions. Other sources considered were those that would arise from a sudden shearing displacement or from microcracking.

Experimental Considerations

It was assumed initially that high fidelity of the acoustic disturbance measurements would be required in order to differentiate adequately between the several sources being considered. For this reason, a laser interferometer system was used at first as a means to detect acoustic emission from crack growth. However, for the particular source types being considered, it was determined that only the magnitude and direction of the initial arriving point of the waveform was required to differentiate between these sources. Consequently, even moderate bandwidth piezoelectric detectors could be used so long as their "footprint" on the test specimen surface was sufficiently

small to permit localization of the crack source. - For the data collection process, therefore, Valpey-Fisher Model 97 pinducers were used as acoustic emission detectors. Test specimens were one inch square notched double cantilever blocks of 7039-T6 aluminum alloy. Six transducers were mounted on the test specimens as illustrated in Figure 1. Prior to testing, calibration of the transducers was carried out by pulsing the specimen with the output from a Nd:YAG laser at the location marked L in the figure. The laser produced a 10 ns pulse, delivering about 10 mJ of laser light. The target area was marked with black marker in order to produce ablation at the illumination site. Signals from the pinducers were collected and digitized and normalized for their responsivity. Immediately after calibration, a mixture of 50% by volume 3.5% NaCl and 50% by volume 3% H₂O₂ was added drop-wise into the crack area. Acoustic emission measurements were carried out over 50-hour time period in which cracks were observed to grow approximately 2 inches. Waveforms from each of the six transducers were digitized and recorded when triggered by an acoustic emission event.

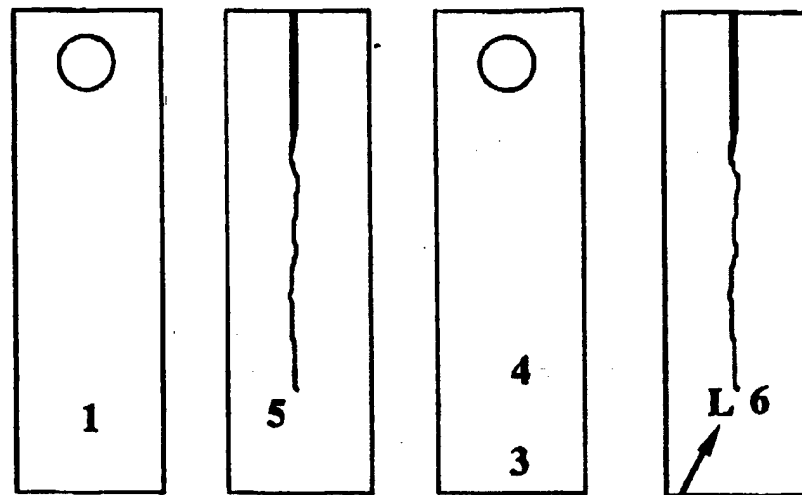
Results and Discussion

In a typical 50-hour period, over 125 events were recorded. The arrival times at each transducer for each recorded event were used to compute source locations for each event. Those events where the crack front was computed to be most equi-distant from all transducers were used for final amplitude analysis. Again, full details of the data analysis are given in Mr. Buckley's thesis. In summary, however, it was clear from examination of the normalized theoretical amplitudes of the key records in the data sets that the nature of the source had to be one of rapid dipole forced generation. A likely mechanism for crack growth, therefore, under anodic dissolution would be that the corroded material near the crack tip would leave weakened areas that would preferentially fracture. The weakened areas in the 7039 alloy might be composed of material left behind after dissolution of anodic precipitates including MgZn₂. This analysis agrees with mechanisms proposed by other investigators as well. Thus, it is concluded that the primary mechanisms for environmentally assisted cracking in 7039-T6 alloy can be attributed to anodic dissolution. Acoustic emission analysis was able to produce quantitative results which support the hypothesis of early investigators who did not have the benefit of real time data as provided by acoustic emission technology.

Presentations

P. F. Buckley, "Acoustic Emission of Stress Corrosion Cracking of High Strength Aluminum Armor Alloys," presented at the May 1995 Acoustic Emission Working Group Meeting, Langley, VA.

P. F. Buckley, "Acoustic Emission of Stress Corrosion Cracking in High Strength Aluminum: Theory and Practice," presented at the November 1995 Society of Engineering Science Conference, New Orleans, LA.



Laser Ablation Location

- 1 = [0.5, 0.0, 0.5]**
- 2 = [0.5, 0.3, 0.0]**
- 3 = [0.5, 1.0, 0.2]**
- 4 = [0.5, 1.0, 0.7]**
- 5 = [1.0, 0.4, 0.5]**
- 6 = [0.0, 0.4, 0.5]**
- L = [0.0, 0.4, 0.5]**

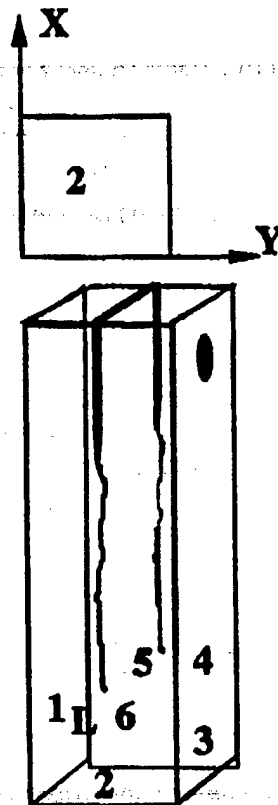


Figure 1. The location of the respective pinducers and the laser ablation site on the double cantilever beam specimen.

Integrity and Effectiveness of Conversion Coatings

Introduction

This research has examined the effectiveness of six non-chromate conversion coatings on aluminum armor alloys 5083, 7039, and 2519. Evaluation included salt fog, cyclic salt spray, wet adhesion, and electrochemical impedance spectroscopy on both painted and unpainted test panels. Large differences in behavior were noted between the salt fog data obtained on unpainted panels and the cyclic salt spray data obtained on painted and scribed panels.

Avoiding corrosion of metallic components used in military equipment has always been a difficult task owing to the harsh nature of the battlefield and extreme environments encountered around the globe. Over the years, many protective schemes have been devised. Of these, chemical treatments containing hexavalent chromium (Cr^{+6}) have been one of the most effective and commonly implemented protective measures. Unfortunately, over the last few decades it has been determined that Cr^{+6} poses a significant health risk. It is a known human carcinogen. The Environmental Protection Agency has continued to press for reductions in the use of hexavalent Cr and improved processing techniques to eliminate Cr^{+6} from the waste stream to reduce the serious threat to personnel and the environment. Thus, the Army is striving to reduce, or even eliminate, its dependency on the use of hexavalent chromium.

To accomplish this, the U.S. Army Research Laboratory (ARL) Weapons and Materials Research Directorate developed and executed a research program under the auspices of the Department of Defense Strategic Environmental Research and Development Program (SERDP) to examine commercially available non-chromate alternatives for protection of aluminum alloys. In parallel with this effort, Johns Hopkins University, through a grant from the Army Research Office, has performed advanced electrochemical testing and modeling of these coating systems. The combined ARL/JHU program provides the spectrum of tests necessary to properly evaluate the coatings and provide insight for future development. These tests included salt fog, cyclic salt spray, adhesion, and electrochemical impedance spectroscopy.

This report will discuss the overall findings of the program, which includes work by ARL (funded through SERDP) and by JHU (funded through the ARO grant).

Experimental Considerations

Thirteen vendors of non-chromate coatings were asked to coat test panels. Of these, four vendors (for a total of six non-chromate coatings) agreed to have their coatings evaluated. For control purposes a chromate conversion coating and a grit blasted condition were also included. Approximately 300 aluminum panels (nominally 10 cm x 15 cm x 0.6 cm) of alloys 2519-T87, 7039-T64, and 5083-H131 were machined from rolled armor plate stock and sent to vendors and Army depots for coating application. Twelve panels for each conversion coating/alloy combination were prepared. From each set of 12 panels, 5 were painted with an epoxy primer and topcoat, 3 panels were coated with the epoxy primer only, and 4 panels were left in the conversion coated state.

Salt fog testing was used to evaluate conversion coated panels that were left unpainted. Two panels of each alloy/conversion coating combination were tested in accordance with ASTM B11, MIL-C-81706, and MIL-C-5541E. The panels were visually monitored for pitting, general corrosion, and staining. Any uniform pitting beyond one or two random pits was considered a failure. The panels were all photographed prior to testing, upon significant observations, and at failure (or the suspension of the test at 1200 hours).

A cyclic corrosion test chamber (CCTC) was used to evaluate painted test panels. For each alloy/conversion coating combination tested, four panels were subjected to CCTC testing; two were coated with the epoxy primer only, while the other two panels were both primed and topcoated with CARC. These panels were "X" scored using a static load of 5 kg applied with a hardened steel scribe. The scribed panels were placed into the chamber and tested with a modified form of GM Standard Test 9540P, Method B to provide a more realistic accelerated environmental test than conventional salt fog. A concentrated 5% NaCl test solution was used in place of the standard 0.9% NaCl + 0.1% CaCl₂ solution called for by 9540P. The 9540P test consists of 18 separate stages which include the following: saltwater spray, humidity, drying, ambient, and heated drying. The environmental conditions and duration of each stage for one complete 9540P cycle are given in Table 1. Again, the panels were all photographed prior to testing, upon significant observations, and at the suspension of the testing (100 cycles).

Paint adhesion for both primed and topcoated panels was determined using a wet adhesion test (Method 6301 of standard MIL-C-81706). In this test, a standard adhesive tape is used to check adhesion on painted specimens after soaking for 24 hours in distilled water. After soaking, each panel is removed and then quickly dried. Two parallel scribes one inch apart are made within the first minute after removal. Tape is uniformly applied across the scribes and then immediately removed. Upon removal, any evidence of paint separation is noted by visual observation of both the panel and the tape. MIL-C-81706 describes adhesion based on a pass or fail system. To receive a "pass" rating, there must be no separation of the paint from the substrate or between layers of the paint. Additionally, we also used a more detailed rating in accordance with ASTM D-3359.

EIS tests were performed with a two-phase lock-in analyzer, a potentiostat/galvanostat, and a personal computer. Periodic measurements were taken for samples exposed to 0.5 N NaCl solution at room temperature at their corrosion potential (stabilized within one hour) over the frequency range of 100 KHz-0.01Hz for a period of up to 28 weeks. The single sine technique was utilized, with a sinusoidal potential impressed upon the open circuit corrosion potential of the substrate (-0.930 V vs. SCE). The applied amplitude depended on the presence of organic primers and topcoats. Amplitudes of 5, 15, and 80mv were utilized for specimens that were only pretreated, pretreated + primed, or pretreated + primed + CARC topcoated respectively. The area exposed for each EIS measurement was 6.3 cm². Generally, EIS tests were performed in duplicate, and only areas without visually detectable defects were selected for exposure to chloride solutions. The collected data were plotted and evaluated in Bode and Nyquist formats. The Bode formats display the magnitude ($\log |Z|$) and phase angle (θ) of the impedance as a function of applied frequency ($\log f$). The total impedance of the specimen, defined as the $\log |Z|$

value at 10 MHZ in the Bode magnitude plot, was also plotted as a function of exposure time for comparison of the effectiveness of each coating system.

Results and Discussion

Detailed results of these studies have been presented in the paper cited below. What follows is a summary of those results.

Salt fog testing examined the degree of uniformity and porosity of the oxide layer and gave general information about the barrier properties of the conversion coating. The results indicated that on one pretreatment (including chromate) was successful on all three alloys. This is especially important for applications where no organic coatings were subsequently applied.

The electrochemical impedance testing provided a good measurement of the effectiveness of the "barrier" properties of each coating system. Most of the non-chromate conversion coatings performed well in this capacity, and most exceed the performance of the chromate controls. Even on alloy 2159, where the presence of Cu could be expected to reduce the uniformity of the pretreatment, good barrier properties were maintained for the 100-plus day exposure. This hypothesis is strengthened by the observation that none of the non-chromate pretreatments nor the chromate controls showed any non-scribe related failures in the 9540P testing through 84 cycles (for all alloys with primer + topcoat). So, from a barrier coating perspective, many of the non-chromate pretreatments provide satisfactory results.

The adhesion tests indicated that most of the non-chromate coatings provided good adhesion of the organic primer and topcoat. The exceptions to this rule occurred for pretreatments NC1 and NC3. The catastrophic adhesion failure of NC3 on all three alloys when only a primer was used indicates that the surface formed during the pretreatment was not stable upon exposure. Adding a topcoat effectively sealed the surface and limited the degradation that was allowed by the primer and, therefore, improvements in adhesion were seen. The adhesion failure of NC1 on 5083 is probably a direct result of the natural corrosion resistance of this alloy; therefore, the reaction kinetics (i.e., corrosion rate) during the pretreatment process are much slower. Longer pretreatment steps may improve the adhesion in this case.

Finally, the ability of the pretreatment to retard corrosion at scratches and other holidays can drastically affect the performance of coating systems in the field. Army systems are especially prone to incidental damage of coatings, so this consideration is vitally important. The chromate conversion coating consistently performs well on all three alloys for both the primer only and primer + topcoat conditions. While several of the non-chromate coatings gave adequate protection on 5083 and 7039, the chromate pretreatment was distinctly superior on 2519. Thus, despite the fact that many of the non-chromate based coating schemes show "barrier" properties that exceed the chromated control panels, the ability of the chromate to inhibit corrosion at the scribed area is the critical factor that allows chromate based conversion coatings to perform so well on many different alloys and in many environments.

The ability of chromate to inhibit corrosion at coating defects must not be overlooked. Most of the developers of new non-chromate based conversion coatings are striving to achieve the 336 hour salt fog resistance required by the qualification standard of MIL-C-81706. It must be stressed that this level of performance might be attained with an effective "barrier" conversion coating that might perform miserably at coating defects. NC1 is an example of an organic conversion that operates in this manner. NC1 performs relatively well in salt fog on 2519, but when scribed and subjected to the cyclic corrosion test, undercutting appears at early stages.

The poor results of NC1 in the cyclic tests on alloy 2519 points out a fact that is too often forgotten: *MIL-C-81706 is a standard for chromate conversion coatings* and should not be considered a performance specification sufficient for any non-chromate alternative. Since the Army (and the rest of the Department of Defense) is currently replacing military specifications with performance specifications, it will be crucial to assess which factors are critical to the performance of the entire coating system. It is our opinion that improved cyclic corrosion testing (such as GM9540P) should be used to replace the salt fog testing in the qualification portions of MIL-C-81706 for both chromate and non-chromate conversion coatings. A statistical analysis of salt fog data has shown negative correlation coefficients when compared to fielded, on-vehicle testing conducted by auto manufacturers, while GM9540P and other cyclic tests have consistently produced correlation coefficients in excess of 70%. After improved performance tests are adopted for qualification, salt fog testing will remain a beneficial quality control test. Further, different performance standards may be needed for conversion coatings that will not be subsequently topcoated (for both chromate and non-chromate coatings), as their performance requirements are inherently different. Therefore, the 336 hour salt fog resistance should not be viewed as the ultimate goal for new non-chromate conversion coatings.

Despite the poor performance of the non-chromate coatings on 2519 (and 2024 in the NCMS study), the good performance on the other alloys studied should not be overlooked. It is apparent that for many applications, non-chromate coatings will give adequate corrosion protection, and we will continue to advocate their use whenever possible.

Conclusions

- Several non-chromate conversion coatings performed well on alloys 7039 and 5083, as demonstrated through the cyclic corrosion testing, salt fog, adhesion, and electrochemical impedance spectroscopy studies.
- The chromate conversion coating gave superior corrosion protection on 2519 due to its ability to retard undercutting at coating holidays.
- The magnitude of the impedance at 0.01Hz, $|Z|$, gives an indication of the barrier properties of the coating system. It does not, however, reflect the ability of chromate conversion coatings to inhibit corrosion at coating defects (when areas free from defects are examined).

- The currently military specifications for chromate conversion coatings should not be directly applied to non-chromate coatings. We recommend that a performance based specification based on one or more cyclic corrosion tests be adopted. Salt fog testing should be used only as a quality control test.

Publications

B. E. Placzankis, J. H. Beatty, J. V. Kelley, and L. A. Krebs, "Evaluation of Non-Chromate Conversion Coatings on Aluminum Armor Alloys," *Corrosion 97*, NACE International, 1997.

Table 1**Interval Statistics per Cycle of GM 9540P Method B**

Interval	Description	Time (min)	Temperature (+/-3C)
1	Ramp to Salt Mist	15	25
2	Salt Mist Interval	1	25
3	Dry Interval	15	30
4	Ramp to Salt Mist	70	25
5	Salt Mist Interval	1	25
6	Dry Interval	15	30
7	Ramp to Salt Mist	70	25
8	Salt Mist Interval	1	25
9	Dry Interval	15	30
10	Ramp to Salt Mist	70	25
11	Salt Mist Interval	1	25
12	Dry Interval	15	30
13	Ramp to Humidity	15	49
14	Humidity Interval	480	49
15	Ramp to Dry	15	60
16	Dry Interval	480	60
17	Ramp to Ambient	15	25
18	Ambient Interval	480	25

Compliant Smart Materials

Senior Investigators: A. S. Douglas and K. T. Ramesh
Technical Point of Contact: P. Blanas

Objectives

Near-Term

- To develop the experimental techniques required to characterize the interaction between large mechanical deformations, forces, and electric fields which characterize the piezoelectric performance in thin compliant smart materials.
- To model these tests in order to obtain quantitative information on deformation, stresses, and electric potentials.

Long-Term

- To characterize full the thermo-visco-elastic and piezoelectric characteristics of polymer based piezoelectric composite materials.
- To establish models of piezoelectric composites which will predict the performance of a sensor given the microstructure (even for large deformations). This will serve as a sensor design and optimization tool.

Research Accomplishments

We have completed development of the experimental techniques required for mechanical and electromechanical characterization of thin compliant smart materials. Some refinement of the techniques is still necessary for measurement of the piezoelectric response, including the evaluation of internal phase differences within the equipment and determination of the effect of a wider frequency range. We now have the experimental facilities necessary for poling of the piezoelectric composite, and for measurement of the signal from the sensors subjected to known mechanical excitations. The composites and the sensors continue to be delivered to us directly from the University of Wales.

The viscoelastic and piezoelectric properties of 0-3 composites consisting of Ca-modified PbTiO_3 particles in P(VDF-TrFE) and Epon828 matrices have been investigated. The frequency response of these composites with ceramic volume fractions between 40% and 673% were studied. As expected, the composites behave more stiffly as the frequency increases. The composites also become stiffer with increasing amounts of ceramic; however, the stiffness is dominated by the matrix at ceramic volume fractions below approximately 60%. The loss tangents of the composites tested were generally larger than those of the matrix materials, indicating possible interface losses.

Analytical and computational models have been shown to predict the storage moduli of the composites fairly well. However, both models predict a decrease in the loss tangent with increasing amounts of ceramic, whereas the experimental results show an increase in the loss tangent. This is possibly due to the perfect bonding assumptions inherent in the models. We have shown computationally that the effect of the interfaces on the viscoelastic properties of the composites may be to increase the loss tangent.

P(VDF-TrFE)/Ca-modified PbTiO₃ composite films have been poled successfully and our results show that the piezoelectric coefficients of these composites are complex and strongly dependent on frequency. The piezoelectric response is presently being investigated more thoroughly, particularly with respect to the effects of frequency and ceramic volume fraction. Thermal effects will also be considered.

A paper on these results will be presented at the SPIE Smart Materials and Structures Conference in San Diego.

Research Interactions

ARL Personnel

Since Dr. Takis Blanas (ARL) is now working at Johns Hopkins, frequent interaction is easily accomplished.

Other Project Collaborators

In October 1996, we were visited by Dr. Dilip DasGupta and Mr. Matthew Wenger of the University of Wales in Bangor. Mr. Wenger spent a month with us accomplishing a substantial transfer of knowledge with Mr. Marra, as well as constructing and evaluating the performance of several sensors in composite plates.

Publications

Marra, S., Ramesh, K. T., and Douglas, A. S., "Mechanical Properties of Compliant Piezoelectric Composites," *Smart Materials & Structures*, SPIE, 1997.

Interface and High Temperature Property Measurements for Metal Matrix Composites

Senior Investigators: M. Rosen and J. B. Spicer
Technical Points of Contact: E. S. Chin and J. M. Wells

Objective

The main program objective was the characterization of the microstructural development of micromechanical interactions between matrix materials and reinforcement agents in metal matrix composites (MMCs). By understanding this development, important information about the processing of MMCs can be used to interpret and improve their performance. Linking micromechanical models of matrix/reinforcement interactions to bulk and interface macroscopic measurements of elastic properties and ultrasonic attenuation, information about the overall performance of the material may be related to the micromechanical behavior of the matrix/reinforcement interface.

Research Accomplishments

In support of the main objective, the various tasks of the program resulted in specific accomplishments which include the following for the past year:

- Preparation and ultrasonic characterization of thermomechanically processed (TMP) discontinuously reinforced aluminum (DRA) MMC materials
- Preparation and ultrasonic characterization of aluminum/17.5% SiC MMC materials
- Construction of experimental apparatus for the real-time ultrasonic investigation of materials undergoing thermal processing
- Refinement of experimental apparatus for the laser generation and laser detection of ultrasonic waves in MMCs.

As part of the first stated accomplishment of the program in metal matrix composites, seven samples from the 6061/ Al_2O_3 system were received for ultrasonic evaluation. The samples were provided by Dr. T. McNelley of the Naval Postgraduate School (NPS). These composites consisted of a 6061 aluminum alloy matrix which was discontinuously reinforced with alumina (Al_2O_3). After the initial casting of the metal matrix composite, thermomechanical treatments of the material were performed at NPS in which plastic deformation at temperature was accomplished using an extrusion operation.

Owing to the matrix/reinforcement composition and to the processing operations, significant variations of the ultrasonic properties were expected. First, the composition of the composite (the volume percent content of alumina - v/o Al_2O_3) should have a direct effect on the

sonic velocities owing to the modulus differences between the aluminum matrix and the alumina reinforcement. According to simple rules of mixture, which hold reasonably well for low Al_2O_3 , the ultrasonic velocities should increase linearly with volume percent since the moduli of alumina are significantly higher than those for aluminum alloys. Secondly, compositional variations should also yield variations in the ultrasonic attenuations owing to impedance mismatches between the matrix and the reinforcement; however, the attenuations depend strongly on both the distribution and the morphology of the reinforcement (brought about by thermomechanical processing) as well as on the volume percent.

The seven samples used in this investigation are listed in Table 1 according to the volume percent reinforcement and the percent strain induced during the extrusion process. Conventional, reflecting ultrasonic methods were used to determine the longitudinal wavespeed, the shear wavespeed, the longitudinal wave attenuation and the shear wave attenuation. The appropriate reflecting surfaces were prepared to be flat and parallel to improve the accuracy of all measurements. These surfaces were perpendicular to the extrusion direction or were perpendicular to the longitudinal axis of the sample. The finished sample lengths were between 12.7 mm and 28.2 mm for all samples except for the Extruded - I x sample which was 9.5 mm.

For the measurements of longitudinal waves, a 20 MHz - 0.25" diameter transducer was used. For shear waves, a 5 MHz - 0.5" diameter transducer was used. Ultrasonic velocity measurements were performed using pulse-echo overlap techniques. Ultrasonic attenuation measurements were made using standard methods; however, corrections for diffraction effects to the indicated attenuations were not made.

The results of these measurements are shown in Fig. 1 (A) and 1 (B). In Fig. 1 (A), the ultrasonic wavespeeds are shown as a function of the fractional volume of Al_2O_3 in the composite. The percent strain is indicated next to each point. The uncertainty in each measurement is less than the extent of a given point which indicates that the "scatter" in the data is real and is indicative of variations in the samples examined. Note that the ultrasonic velocities increase linearly with the reinforcement volume percent; this variation is highlighted by the best linear fit which is shown with the data. Note that the unreinforced 6061 material has ultrasonic velocities which are higher than those indicated by the linear fit to the data. Additionally at 10% and 20% reinforcement, the relative velocities as a function of the plastic strain at a given reinforcement are consistent between longitudinal and shear waves. For example, at the 20% level, the wavespeeds for the 4.32 strain sample are higher than those of the 5.32 strain sample. At the 10% level, the longitudinal wave velocities for the 0.0, 4.32 and 5.32 samples are within 0.06% of each other; however, the 2.1 sample is far below the others. Similar results were obtained for the shear wave which shows a 1% variation in velocity among the 0.0, 4.32 and 5.32 samples with the 2.1 sample yielding the lowest shear wave velocity.

These results indicate that significant variation in the longitudinal and shear velocities have been measured for these samples. The correlation of the velocities with volume percent Al_2O_3 has been shown. Additionally, variations with the thermomechanical treatment have been measured; however, the results cannot be correlated definitively owing to the uncertainty concerning actual grain microstructure and/or the small number of samples which have been assessed in this study. The results obtained on this set of samples show definite variations which should be

correlated to actual materials microstructures; however, it may be that these variations are related to the nominal processing conditions in a statistical sense and an analysis using a significant sampling should be pursued.

In contrast, dramatic correlation between the thermomechanical treatment and the ultrasonic attenuation has been observed and is shown in Fig. I (B). In this figure, the longitudinal and shear wave attenuations are shown as functions of the fractional volume of Al_2O_3 . Generally, accurate attenuation measurements are difficult to perform; however, since the attenuation measurements on these samples were obtained under similar conditions, comparisons may be made. Notice that the attenuations for both the longitudinal and shear waves are nearly independent of the reinforcement volume fraction and are in agreement with the attenuations measured for the unreinforced matrix alloy. However, the attenuation of the "as cast" material was too high to observe in this series of measurements. An insufficient number of ultrasonic echoes was observed to make an attenuation measurement within the uncertainty of the other measurements. A lower bound for the attenuation of the "as cast" material was estimated using the number of echoes observed and comparing this number to results for the other materials for which the attenuation was measured with certainty. Clearly, the thermomechanical treatment markedly reduced both the longitudinal and shear attenuations. This reduction may be a result of the modifications of the reinforcing phase morphology and interface condition with the matrix. If the reinforcing phase is elongated along the axis of extrusion, then the effective scattering cross section for waves propagating along this direction would be decreased thereby decreasing the attenuation. If the interface between the matrix and the alumina becomes ultrasonically continuous as a result of treatment, then a reduction in scattering would also be expected leading to reduced attenuation. Measurements of the attenuations perpendicular to the extrusion direction would aid in the experimental analysis. These measurements were not performed.

As part of the second stated accomplishment of the program in metal matrix composites, six samples from the 6092 aluminum/17.5% SiCp system were received for ultrasonic evaluation. The samples were provided by Dr. J. Wells during his tenure at NPS. These composites consisted of a 6092 aluminum alloy matrix which was discontinuously reinforced with silicon carbide particles (SiCp). Thermomechanical treatments of the material were performed at NPS in which plastic deformation at temperature was accomplished using extrusion operations. It is noted that these samples were compositionally identical; the differences among the samples resulted strictly from the thermomechanical processing.

Conventional, contacting ultrasonic methods were used to determine the longitudinal and the shear wavespeeds in these samples. The appropriate sample surfaces were prepared to be flat and parallel to improve the accuracy of all measurements. These surfaces were perpendicular to the extrusion direction or were perpendicular to the longitudinal axis of the sample. Ultrasonic velocity measurements were performed using pulse-echo overlap techniques. Owing to the dimensions of the prepared samples, attenuation measurements could not be performed using standard methods and were pursued using laser ultrasonic methods.

The results of these measurements are shown in Fig. 2 where the ultrasonic wavespeeds are shown for the various composite samples. The sample identification labels are indicated next

to the data points. The uncertainty in each measurement is less than the extent of a given point and, consequently, the values indicated for the wavespeeds may be directly correlated to actual microstructural variations in the samples examined. The interpretation of the data gathered for these samples was not as direct as that given for the Al/Al₂O₃ system owing to limited number of samples available for examination. The most consistent result shown by the data is the increase in the longitudinal wavespeed between the 85/85-A samples in the 85 pair and the 86/86-B samples in the 86 pair. According to J. Wells, the only difference between the samples in each pair was that samples 85-A and 86-B were subjected to a post extrusion heat treatment and water quench which was not performed on the 85 and 86 samples. It is clear that the ultrasonic results indicate the effects of the additional heat treatment; however, it is not clear if these results are statistically significant within the overall variations which occur during processing.

The third and fourth accomplishments of the program were related to improvements in ultrasonic instrumentation which were pursued during the past year. As was mentioned in the description for the 6092/17.5% SiCp measurements, attenuation measurements on these samples could not be performed using traditional techniques owing to the small, restrictive sample dimensions. However, the investigation of the ultrasonic properties of these MMC samples could be achieved conveniently using laser ultrasonic methods since the effective transducer size may be adjusted using optical lenses to focus the generation and detection laser beams. These methods are schematically represented in Fig. 3. A pulsed laser (pulse duration ~20 ns, pulse energy ~40 mJ) was used to irradiate the surface of the MMC sample (shown with reinforcement) thereby inducing ultrasonic transients in the material. These transients were sensed in transmission using an interferometric transducer. A laser ultrasonic waveform showing the ultrasonic signal amplitude as a function of time is shown in Fig. 3 for a sample from the 6092 Al/7.5 v% SiC particulate reinforced composite series. A thorough investigation of these materials using the laser-based ultrasonic instrument was not performed; however, it was demonstrated that the laser-based methods could be used to investigate the MMCs in this program if the measurements were required.

Conclusions

Contacting ultrasonic measurements on the aluminum matrix 6061 discontinuously reinforced with alumina have demonstrated that the ultrasonic velocities, longitudinal and shear, are functions of the reinforcing phase volume percent. Other variations of the velocity with the thermomechanical treatment have been observed; however, correlation of these variations with particular microstructural variations has not been obtained. Both the longitudinal and shear wave attenuations have been shown to be strong functions of the thermomechanical treatment which occurs between the "as cast" state and subsequent states.

Ultrasonic measurements on the aluminum matrix (6092) 17.5% SiCp reinforced MMC showed correlation between the longitudinal wavespeed and the heat treatment of these materials. However, these results may or may not be significant in elucidating the effects of processing on microstructure given the variability of the MMC heat treatment and the sensitivity of the ultrasonic measurements.

Finally, a successful demonstration of laser ultrasonic measurements in the 6092/SiC MMC system was performed. Many composite systems respond poorly to laser ultrasonic methods; however, it has been shown that such measurements may be performed with a sufficient degree of accuracy to allow for materials characterization of this system.

Summary

It is clear that the results obtained in this program demonstrate that ultrasonic methods may be used to nonintrusively gauge variations in microstructure which result from MMC processing; however, the definitive relation of the microstructural variations to ultrasonic properties was not achieved owing to program redirection.

Sample Description	Volume Percent Al_2O_3	Strain
6061 - Unreinforced	0	0.0
As Cast	10	0.0
Extruded - 1x	10	2.1
18-10-10	10	4.32
1-10-1	10	5.32
23-20-4-2	20	4.32
5-20-2-2	20	5.32

Table 1: Listing of metal matrix composite designations with the associated reinforcement levels and induced strain during mechanical deformation.

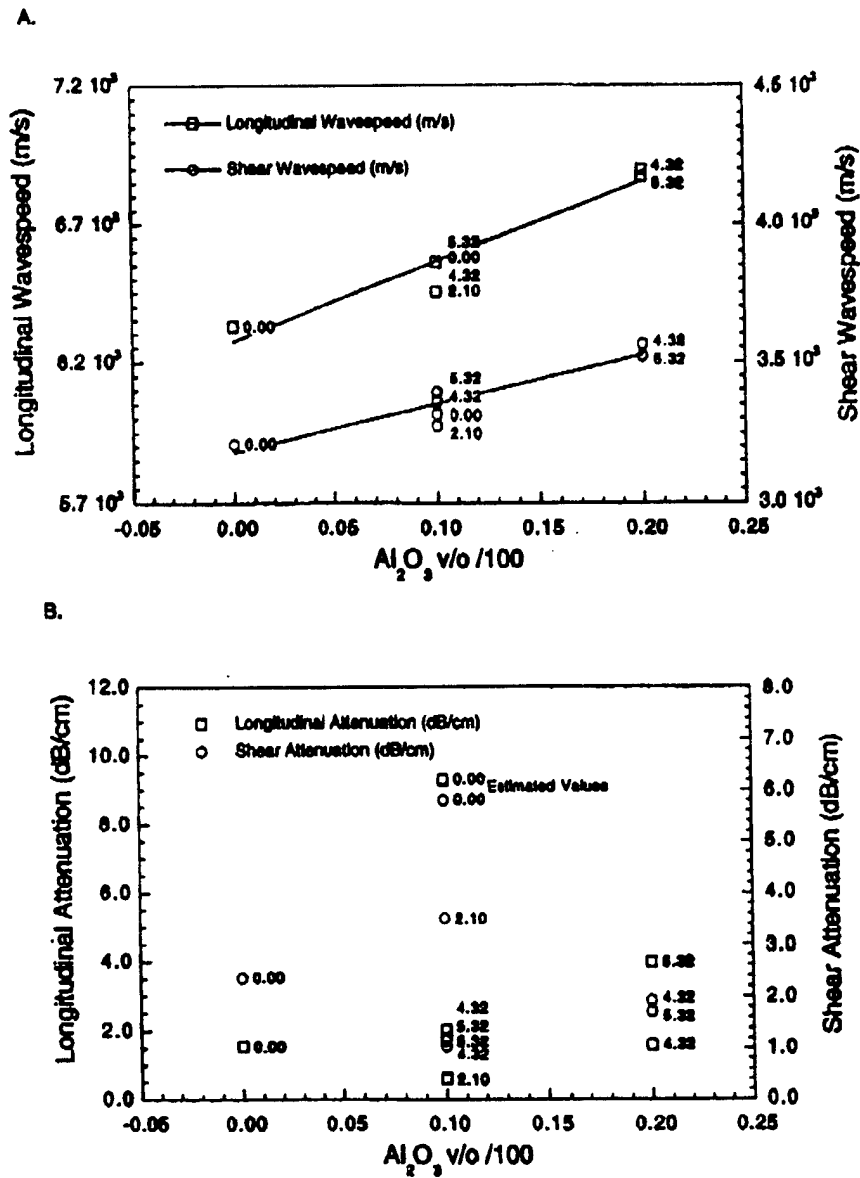


Figure 1: Longitudinal/shear wavespeeds and attenuations for NPS thermomechanically processed 6061/ Al_2O_3 metal matrix composites. Wavespeeds and attenuations are shown as a function of the v/o alumina and are labeled by the plastic strain induced during extrusion.

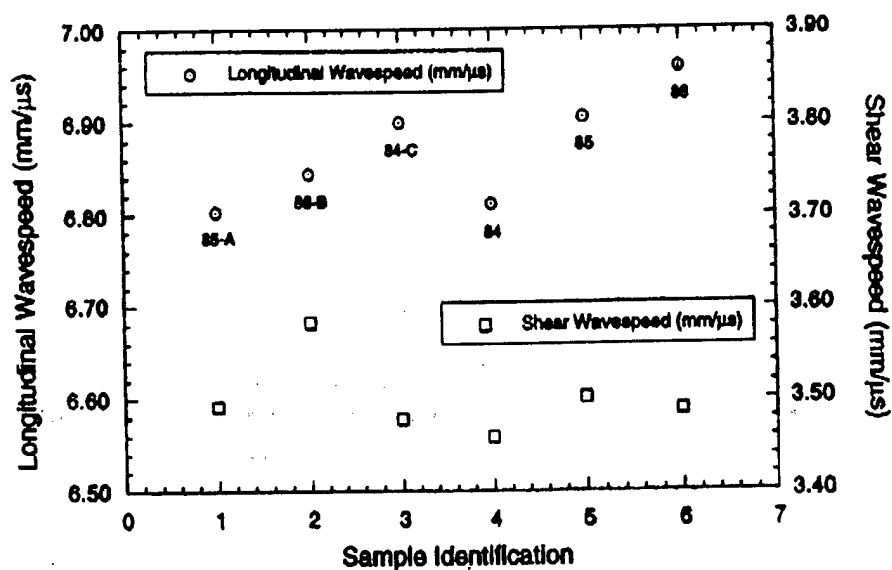
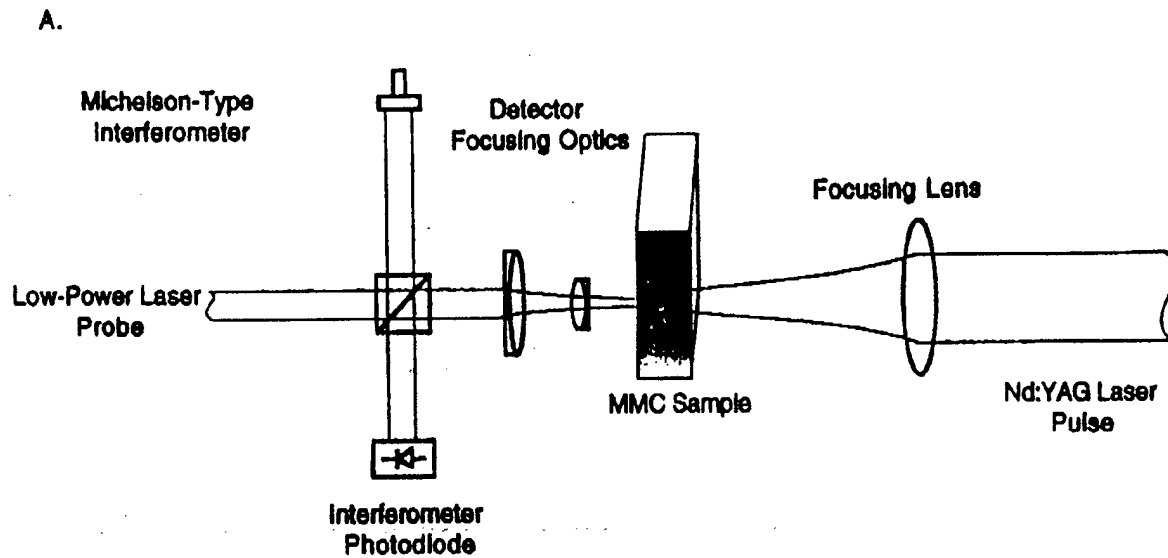


Figure 2: Longitudinal/shear wavespeeds for NPS thermomechanically processed 6092/17.5% SiCp metal matrix composites. Wavespeeds are shown and are labeled according to the sample identification number.



B.

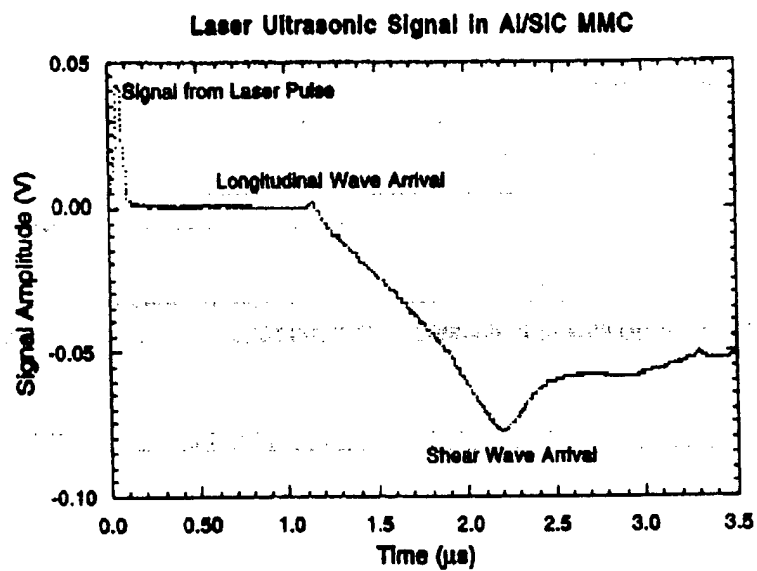


Figure 3: A. Experimental apparatus for laser ultrasonic measurements on MMC's.
B. Laser ultrasonic waveform obtained on a 6092 /17.5% SiCp metal matrix composite sample.

Adiabatic Shear Localization in Body-Centered Cubic Metals

Senior Investigators: K. T. Ramesh and K. J. Hemker
Technical Points of Contact: D. Dandekar and B. Dowding

Objectives

Near-Term

- The development of a high-rate, high-temperature capability for the measurement of the dynamic thermomechanical behavior of *bcc* metals.
- High-rate thermomechanical characterization of a model *bcc* metal with *thermophysical* properties that are conducive to shear localization. First, completion of the characterization of pure polycrystalline and single crystal tungsten.

Long-Term

- The development of a clear picture of the microscopic processes associated with high-rate deformations in *bcc* metals.
- Determination of the distinctions between the microscopic mechanisms involved in the high-rate localized deformations of *bcc* and *hcp* metals. The intent is to develop criteria for microstructural modifications that lead to easier adiabatic shear localization.

Research Accomplishments

We have completed construction of the high-temperature, high-rate capability using HgCdTe photodiodes for the high-speed temperature measurement and IR spot heating and temperature controlling equipment for rapid heating of specimens in the compression Kolsky bar. The high-speed IR temperature measurement system uses a photovoltaic MCT diode with the associated IR optics; we have used this to measure temperature rises during dynamic deformations in aluminum and titanium specimens. Comparison of our results with those of other workers indicates that we must improve our calibration techniques to some extent; we are, therefore, in the process of developing improved calibration procedures.

We are currently performing the high-rate characterization of pure polycrystalline vanadium in the annealed condition. Quasistatic (MTS) compression and the compression Kolsky bar have been used to cover a range of strain rates from 10^{-4} to $6 \times 10^3 \text{ s}^{-1}$. The overall response of the vanadium is typical of a *bcc* metal in terms of rate-hardening and strain hardening, but the material also manifests a dynamic recovery behavior with increasing temperature. Vanadium is also observed to manifest extremely stable deformations, with compressive strains of $>100\%$ easily achieved with no indication of localization. This work is being submitted to the DYMAT97 conference and will also be submitted for publication in the archival literature.

We are proceeding to perform the microstructural examinations using TEM of the deformed vanadium specimens to determine the microscopic deformations mechanisms within the material.

Nondestructive Characterization of Polymer Matrix Composite Materials

Senior Investigator: R. E. Green, Jr.

Co-Investigators: J. W. Wagner, J. B. Spicer, J. M. Winter

Technical Points of Contact: Richard Shufford and Ralph Adler

Objective

The objective of this research is to develop and apply optical, electromagnetic, air-coupled acoustic technology, holographic interferometry, high resolution microfocus x-ray radiography and computer assisted tomographic imaging to optimized measurement of the mechanical properties and structural state of polymer matrix composite structures, including lay-up and fiber orientation, and to monitor the chemical and mechanical degradation of military structures made from these composites while in service.

Research Accomplishments

In order to satisfy this objective, research has been conducted to develop and apply non-contacting laser systems, electromagnetic acoustic transducers (EMATs), and air coupled ultrasonic technology. The methods used were: (1) hybrid laser generation/EMAT detection ultrasonic systems; (2) laser generation/laser detection ultrasonic systems (including holographic methods); (3) air-coupled ultrasonic systems; (4) hybrid laser generation/air-coupled detection ultrasonic systems. Five sets of composite panels and several pre-pregs were nondestructively tested using the above methods. The first set was six 16-layer AS4/epoxy thermoset panels with a variety of intentionally introduced void contents. The second test specimen was a thermoplastic tow-placed panel. For this panel, individual AS4/PEKK tows were placed under varying process conditions on a press-consolidated, 16-layer, quasi-isotropic substrate. The third test set was tow-placed panels consisting of 8 layers each of AS4/PEKK of IM7/AvimidK3B material with a variety of lay-ups. The fourth set was samples of AFR 700 high temperature material from Wright-Patterson AFB. The fifth set was AS4/3501-6 graphite/epoxy panels manufactured by Johns Hopkins graduate students at the Naval Surface Warfare Center, Annapolis, MD. The pre-preg investigated was from this latter material also.

A completely new design laser generation system capable of generating discrete narrow band frequency ultrasound rather than the broad frequency band ultrasound generated by conventional laser pulses was optimized. This multi-element laser system was composed of ten Q-switched Nd:YAG cavities with a common power supply and timing electronics. The timing circuit allowed the lasers to be fired with a large variety of delays. Turning mirrors were used to direct the infrared light pulses through a cylindrical lens to the surface of the test specimen. This system was implemented to serve either for laser generation/EMAT detection or for laser generation/laser detection of ultrasound. The ten laser system was also operated as a phased array. This laser array system was applied for the experiments involving laser generation/laser detection of ultrasound.

The first experiments were performed on two of the 16-layer quasi-isotropic AS4/epoxy thermoset panels. The two test panels selected were composite panel #2(CP2), which was laid up without any intentional porosity, but with simulated delaminations, and composite panel #4(CP4) which contained intentionally created porosity. The simulated delaminations and the porosity difference were easily imaged. For the second set of experiments, which was performed on the thermoplastic AS4/PEKK tow placed panel, differences were found between well-bonded (tow #13) and poorly bonded (tow #11) regions. Certain regions of this panel were found to contain voids and regions of poor bonding under the top tow layer. The laser ultrasonic signatures containing higher frequency components correspond to regions of the panel where there was good adhesion between the tow placed layer and the substrate. The third set of experiments was conducted on AFR 700 high temperature composite material from Wright-Patterson Air Force Laboratory. A sequence of waveforms recorded on the opposite side from generation (through transmission) as the receiving interferometer laser probe moved from a position directly beneath the source (epicenter) to several off-epicenter positions at progressively increasing distances was recorded. A significant attenuation of the high frequency components of the ultrasound signal was observed.

After completion of the initial effort to optimize the air-coupled ultrasonic C-scan system, it was used to successfully perform C-scans on several composite specimens. C-scans were performed on AS4/3501-6 pre-impregnated graphite/epoxy lamina using a frequency of 0.5 MHz. Both transducers were coaxially aligned perpendicular to the sheet, focused on either side into the surface, and stepped in 0.02 inch increments. Darker regions in the resulting images indicated higher attenuation, which in most cases correlated with a lack of infiltration of epoxy resulting in degrading the quality of the pre-preg. The results also showed that the pre-pregs were very inhomogeneous primarily due to uneven distribution of resin. Air-coupled C-scan images were also obtained from 16-layer quasi-isotropic AS4/epoxy thermoset panels. It was very easy to image a one-inch square of Tedlar release film shim intentionally placed several layers down to simulate a delamination. All panels tested exhibited inhomogeneity, and all intentionally introduced defects as well as porosity were easily imaged.

In addition to the non-contact ultrasonic systems, a completely new technique called full-field holographic interferometry imaging of acoustic displacements was optimized and applied to composite structures. One experiment showed that this technique could be used to successfully image the surface displacements due to ultrasonic wave propagation in a graphite/epoxy plate. Both the anisotropy of the lay-up and the presence of a delamination were evident in the resulting holographic image.

The most recent effort has been the successful development of a high resolution microfocus x-ray radiographic system for application to composites. This system is now capable of imaging and recording x-ray images at television scan rates. Progress has been made, with the cooperation of researchers at Lawrence Livermore National Laboratory (LLNL), to further modify the system to permit it to perform near real-time computer assisted tomographic reconstruction of three-dimensional volumetric images of composites. In this regard, a new high-resolution computer controlled three-dimensional specimen movement system has been received and will be installed in the near future. Also a silicon graphics indigo work station has been

acquired and loaded with software provided by LLNL to record and display the 3-D images. The system is currently being tested both on simulated and real data provided by LLNL.

Publications and Presentations

"NDE of Polymer Matrix Composites," Robert E. Green, Jr., U.S. Army Materials Research Center of Excellence Program Meeting, Johns Hopkins University. January 25-26, 1995.

"The Johns Hopkins University Center for Nondestructive Evaluation," Robert E. Green, Jr., Seminar at the Army Materials Directorate, Watertown, MA, February 23, 1995.

"NDE of Composites," Tutorial, Robert E. Green, Jr., SPIE Meeting, Oakland, CA, June 6, 1995.

"Nondestructive Characterization of Polymer Matrix Composite Materials," Annual Progress Report, Materials Research Center of Excellence, Cooperative Agreement No. DAAH04-G-0316, January 1996. (36 pages).

"Industry Workshop for Online Composite Process Monitoring," R.E. Green, Jr., National Institute of Standards and Technology, Gaithersburg, MD, April 3-4, 1996.

"Nondestructive Characterization of Polymer Matrix Composite Materials," Robert E. Green, Jr., Army Research Laboratory Meeting, Chestnut Run, Delaware, June 20, 1996.

"Laser Ultrasonic Chirp Sources for Low Damage and High Detectability Without Loss of Temporal Resolution," T. W. Murray, K. C. Baldwin, and J. W. Wagner, submitted to Journal of the Acoustical Society of America.

Diffusion of Vapor Mixtures Through Elastomers

Senior Investigator: T. A. Barbari
Technical Point of Contact: J. M. Sloan

Objective

The objective of this project was to measure the rates at which individual components of a vapor mixture diffuse through polymeric elastomers in order to develop initial structure-property relationships that will guide material selection for service in harsh environments.

Research Accomplishments

A conventional gravimetric vapor sorption balance was linked to an FTIR spectrometer in order to measure diffusion coefficients from the vapor phase using attenuated total reflectance spectroscopy. With both gravimetric and spectroscopic techniques coupled in this manner, diffusion coefficients obtained from the two techniques could be compared. Mutual diffusion coefficients for methyl ethyl ketone (MEK) in polyisobutylene (PIB) were measured with both methods at various solvent activities and temperatures in the range 40-60°C. The concentrations in the polymer were determined from the sorption balance. The diffusion coefficients from the two techniques agree very well. In addition, the diffusivities could be correlated with the Vrentas and Duda free volume model.

Initial diffusion data were obtained with toluene/MEK mixtures in PIB at 50°C. The results indicate that a binary transport model can be used to measure the diffusion coefficient of a faster-diffusing penetrant. In the system studies, MEK diffuses faster and is not affected by the presence of the slower toluene molecules over the compositions examined. The MEK molecules "see" only the polymer as they diffuse. In contrast, a ternary model is required to analyze the toluene data. Toluene molecules "see" an MEK/PIB mixture as they diffuse across the film.

Publications

S. U. Hong, T. A. Barbari, and J. M. Sloan, "Diffusion of Methyl Ethyl Ketone in Polyisobutylene: Comparison of Gravimetric and Spectroscopic Techniques," *J. Polym. Sci.: Polym. Phys. Ed.* (in press).

S. U. Hong, T. A. Barbari, and J. M. Sloan, "Multicomponent Diffusion of Methyl Ethyl Ketone and Toluene in Polyisobutylene from Vapor Sorption FTIR-ATR Spectroscopy," *J. Polym. Sci.: Polym. Phys. Ed.* (submitted).

S. U. Hong and T. A. Barbari, "A Study on Diffusion of Methyl Ethyl Ketone in Polyisobutylene Using FTIR-ATR Spectroscopy." Poster presented at ACS Interdisciplinary Workshop on Polymer Surfaces and Interfaces, October 21, 1996.

Characterization and Modification of Silicon Surfaces at Liquid Surfaces

Principal Investigator: P. C. Searson

Technical Points of Contact: R. Adler and J. Hirvonen

Objective

The objective of this project was to explore techniques for the characterization and modification of silicon surfaces at liquid interfaces. The approach involved the development of a scanning tunneling microscopy for atomic scale characterization and manipulation of silicon surfaces.

Summary

Etching of silicon in aqueous fluoride solutions can lead to almost atomically flat surfaces with a low density of surface states and recombination centers. The final quality of the surface, however, is strongly dependent on the solution composition and pH. Extending last year's effort to apply electrochemical impedance spectroscopy to characterize the interface modification process, we have developed a new method, potential modulated microwave reflectance spectroscopy (PMMRS). With this combination of methods, it is possible to elucidate the processes occurring at the surface during etching. PMMRS is a novel technique that only probes the free carriers in the conduction and valence bands and is, under certain circumstances, not affected by processes involving electrically active surface states or charged transfer. This unique feature makes it possible to separate the energetics of the semiconductor from the surface modification process. Microwave reflectivity versus potential curves in HF solutions demonstrate variation of the flat band potential as a function of pH.

Background

Technological applications for high purity silicon are derived from properties such as the ability to form an insulating oxide layer by chemical or thermal treatment, an optical band gap in the infrared, long minority carrier diffusion length, and the relatively low cost of high quality materials. The interaction of silicon interfaces with HF solutions represents one of the more important methods for surface modification. Examples of processes involving interaction with HF include: oxide removal, hydrogen passivation, porous layer formation, wafer cleaning, electroplating, and chemical etching. Chemical etching of silicon in HF solutions is important for oxide removal and in the formation of stabilized silicon surfaces by hydrogen passivation. Recent work has led to dramatic advances in the understanding of the relationship between etching processes and atomic scale structure. Advances in selective etching based on orientation dependent etch rates have led to widespread use of wet chemistry in microfabrication.

In the semiconductor industry, the continuing decrease in feature sizes has resulted in increasing emphasis on understanding surface properties. Silicon wafers are routinely pretreated in HF solutions to remove residual SiO_2 , resulting in hydrogen terminated surfaces of good

electrical quality. Consequently, it is desirable to have in situ techniques which can be used to monitor the surface modification in contact with HF solutions. During last year's effort, electrochemical impedance spectroscopy (EIS) was used to determine the charge and the potential distribution at the silicon/electrolyte interface by measuring the impedance as a function of potential. However, the determination of the flatband potential and the doping density becomes complicated in the presence of surface states. In addition, at potentials more negative than the flatband potential, the charge transfer impedance dominates the electrical response, and studying the space charged layer becomes increasingly difficult. The PMMRS method developed during this past program year is a novel in situ technique that allows the separation of the space charge and surface processes.

Theoretical Considerations

The microwave reflectivity of a semiconductor is proportional to its conductivity. Small changes in microwave reflectivity in an n-type semiconductor wafer, for example, can be attributed to a corresponding change in the mobile majority carrier concentration. For a wafer of known thickness upon which a varying potential can be impressed, the change in mobile majority carrier concentration is proportional to the space charge layer capacitance and to the amplitude of the potential modulation. For a sinusoidal potential modulation in the depletion region, the application of a more negative applied potential increases the space charge layer capacitance and, in turn, the mobile majority carrier concentration. Thus, an increase in microwave reflectivity is observed. Note that the change in microwave reflectivity will be 180° out of phase with the potential modulation. In fact, this is observed experimentally with the change in reflectivity having a large negative real component and a negligible value of an imaginary component. The equilibration process of the mobile majority carriers in the space charge region of silicon is much faster than the frequency of the potential modulation so that the microwave response is independent of electron transport in the bulk of the material.

Experimental Results

Experiments were performed on 25 ohm-cm, n-type silicon (111). The wafers were cleaned with HF and rinsed in de-ionized water. Ohmic contact was made along the circumference of the back of the wafer. The wafer was then placed in the experimental configuration shown in Figure 1. Employed in the experiment was a rectangular X-band waveguide system with a 60mW, 9.33 GHz microwave source where the microwave field was directed toward the backside of the silicon wafer. Typical amplitudes and frequencies of the potential modulation for the EIS and PMMRS systems were 30mV (rms) at 1 KHz in the deep depletion region and 10mV (rms) at 20 Hz in the surface state regime. PMMRS measurements at potentials more negative than the flatband potential were performed at 30 mV (rms) and 20 Hz. All potentials were measured with respect to the saturated calomel electrode (SCE).

Results

PMMRS and EIS measurements were performed in 1 M HF (pH2) and 0.01 M NH_4F (pH 6.8) with both solutions having the same fluoride ion concentration. Figure 2 shows a semi-

logarithmic plot of ΔR -real and $|\Delta R|$ versus frequency in 0.01 M NH_4F in the deep depletion regime ($U = +0.3$ V). The plot shows that ΔR is virtually independent of frequency. The roll-off at frequencies close to 10^5 Hz is due to the response of the potentiostat. At frequencies below 10 Hz, there is some scattering in the microwave response. As expected, the magnitude of ΔR -real is equal to $|\Delta R|$ implying that ΔR -imaginary is negligible. The anticipated 180° phase shift between the modulating potential and ΔR is confirmed from the fact that ΔR -real is negative.

Figure 3 shows typical Mott-Schottky plots of C^{-2} and ΔR^{-2} versus potential in 1 M HF (pH 2). The flatband potential determined from these results was -0.30 V(SCE). The microwave response over the entire depletion regime compares remarkably well with the capacitance response showing that ΔR is proportional to C_{sc} as was expected. Similar plots in 0.01 M NH_4F (pH 6.8) yielded a flatband potential of -0.40 V (SCE) showing that the flatband potential shifts to more negative values with increasing pH.

Figure 4 shows the capacitance and ΔR versus potential in a 0.01 M NH_4F solution (pH 6.8) in the potential regime where electrically active surface states dominate the impedance response. At potentials between -0.2 V and -0.6 V, the capacitance - potential curve shows a maximum and the capacitance is due to the filling and emptying of surface states. The ΔR curve, on the other hand, shows that the microwave reflectivity method only detects changes in the space charge capacitance and is not affected by the presence of surface states.

The surface state density can be calculated from the capacitance peak and was determined to be $\approx 3.3 \times 10^{11} \text{ cm}^{-2}$. Assuming a Helmholtz layer capacitance $C_H \approx 2 \times 10^{-6} \text{ F cm}^{-2}$, the band edges shift by about 26 mV as the Fermi level moves through the surface states. These results show that the band edges are essentially fixed as the Fermi level is increased from deep depletion to weak depletion.

The ΔR response at potentials negative of the flatband potential was also investigated and the results obtained in 1 M HF (pH 2) are shown in Figure 5. The ΔR curve goes through a maximum close to -0.6 V(SCE), and ΔR subsequently decreases towards zero. This indicates that the modulated applied potential is mainly dropped over the Helmholtz layer at potentials more negative than -1 V. These results also confirm that the microwave response only detects a modulation of the free carrier concentration and is not affected by charge transfer processes. The increase in the ΔR signal in the narrow potential region negative of the flatband potential (-0.3 V) is exponential with an inverse slope of 280 mV/decade. The expected potential dependence of the capacitance for an accumulation layer is 120 mV/decade implying that the applied potential is partitioned over the accumulation layer and the Helmholtz layer in this region. These results show that PMMRS is a unique technique which allows us to probe the accumulation regime of the silicon/electrolyte interface.

Publications

A. Natarajan, G. Oskam, D. A. Oursler, P. C. Searson, "Characterization of the Silicon/Fluoride Solution Interface by In-Situ Microwave Reflectivity," MRS Symposium Proceedings Series: Electrochemical Synthesis and Modification of Materials, Vol. 451, Boston, MA, Dec. 1996.

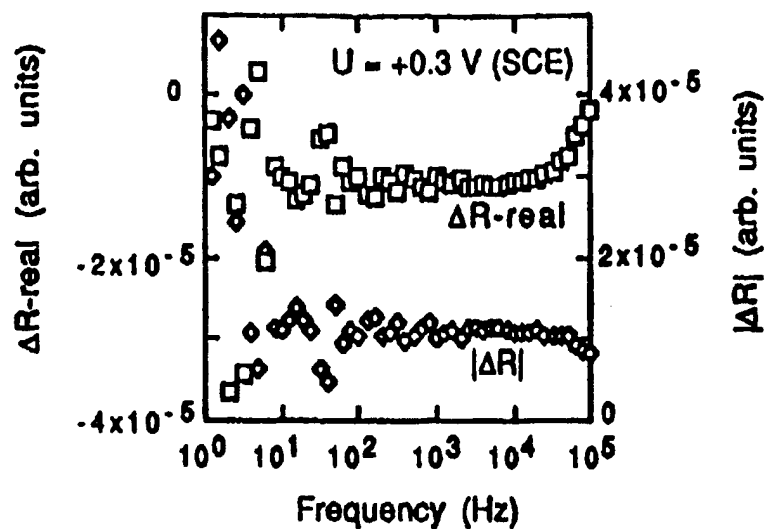


Figure 2. Bode plot of $\Delta R\text{-real}$ and $|\Delta R|$ versus frequency under depletion conditions in $0.01 \text{ M NH}_4\text{F}$ (pH 6.8).

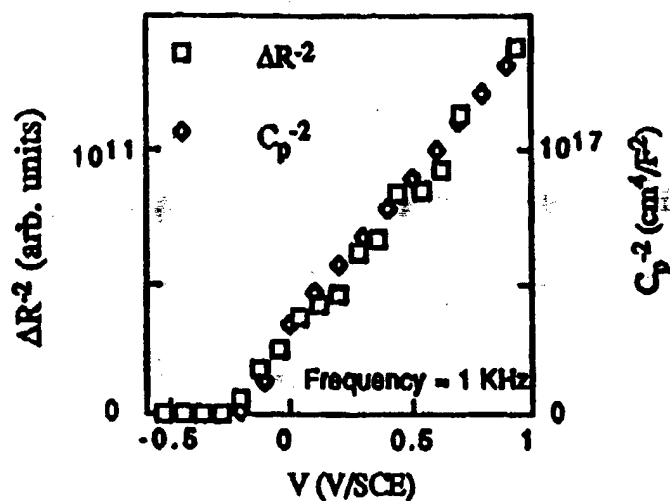


Figure 3. ΔR^2 and C_p^2 versus potential plots in 1 M HF (pH 2). C_p is the parallel capacitance. The scan rate was 3 mVs^{-1} .

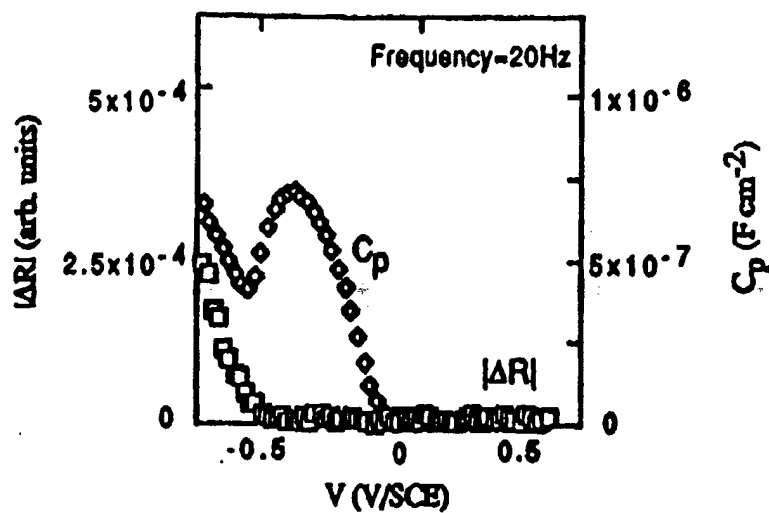


Figure 4. ΔR and C_p versus potential in the surface state regime in 0.01 M NH_4F (pH 6.8). The scan rate was 1 mVs^{-1} .

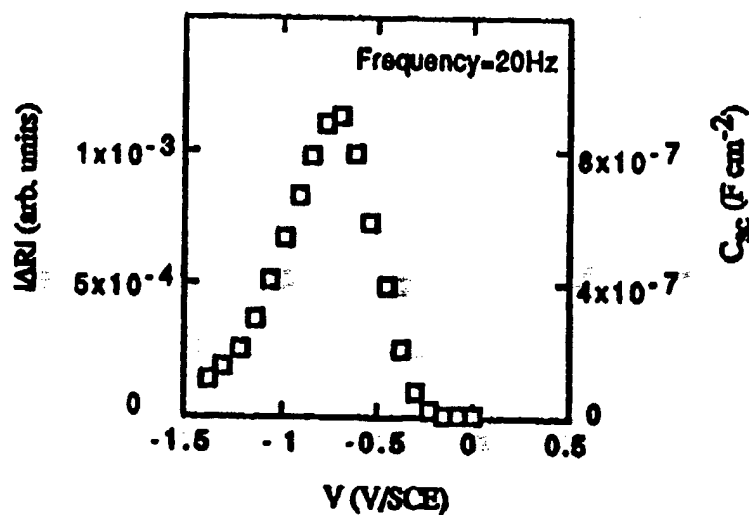


Figure 5. ΔR and C_{sc} (calc.) versus V at negative potentials in 1M HF (pH 2). The magnitude of C_{sc} was determined from equation (3). The scan rate was 3 mVs^{-1} .

Process Monitoring and Control in the Production of Austempered Ductile Iron

Senior Investigator: J. B. Spicer
Technical Point of Contact: J. M. Wells

Objective

The primary objective of the proposed program was to develop real-time sensing and control strategies for the austempering process in ductile cast irons. Acquisition of realtime, in-process information about microstructural evolution in these alloys allows for optimization of the heat treatment thereby resulting in improved materials properties.

Research Accomplishments

Austempered ductile iron (ADI) is a cast iron material which is strong, lightweight and wear resistant compared to steels. The microstructure of ADI is unique to cast irons and consists of acicular ferrite with high-carbon, stable austenite. This microstructure is obtained by a predetermined heat treatment which is based on the precise constituent alloying elements in the iron. If held at the heat treatment temperatures too long, the microstructure transforms to bainite which is undesirable in ADI.

The method pursued under this program by which the ADI microstructure may be interrogated was a laser ultrasonically based technique originally developed for the monitoring of austenitic stainless steels undergoing heat treatment. The basis of the technique is the ability to acquire ultrasonic information (longitudinal wave velocity and attenuation, shear wave velocity and attenuation) while the ADI is being heat treated. It is well known that ultrasonic attenuation measurements are highly sensitive to materials microstructure; however, the reliable acquisition of attenuation information is often precluded by the processing environment imposed by heat treatment operations. Using laser-based methods, it appears that sufficient information about the ultrasonic attenuation may be acquired while the heat treatment process is being performed.

Laser ultrasonic probes have been developed (under separate programs) which are sufficiently stable to allow for continuous ultrasonic monitoring of materials undergoing heat treatment. Using these probes, the heat treatment of aluminum alloys has been monitored. The results of this monitoring indicate that the onset of age hardening may be identified accurately in a range of alloy systems. Using these alternate materials systems, the data acquisition and analysis techniques required for microstructure monitoring have been refined and expanded to allow for more robust analysis of data obtained from ADI.

Unfortunately, cast irons, unlike aluminum alloys and stainless steels, oxidize heavily in air atmospheres during heat treatment yielding non-transparent, surface oxide layers which preclude laser ultrasonic monitoring of the material. A furnace with retort was procured for the heat treatment of the cast irons in controlled atmospheres, and the furnace and retort were modified to

allow for laser ultrasonic monitoring. To date, this furnace has not come on-line for completion of the program.

Laser ultrasonic tests have been performed at room temperature on the ADI in the as-received condition and in the after-heat-treatment condition. The results of these tests indicate that ADI is a suitable candidate for in-process monitoring. The tasks of this program are being carried on with results being forwarded to the Army POC as they become available.